

# Roll-Pitch-Yaw Integrated $H_\infty$ Controller Synthesis for High Angle-of-Attack Missiles

**Byung-Hun Choi\*, Seon-Hyeok Kang\* and H. Jin Kim\*\***

Institute of Advanced Aerospace Technology  
School of Mechanical and Aerospace Engineering  
Seoul National University, Seoul, 151-742, Korea

**Dae-Yeon Won\* and Youn-hwan Kim\***

Division of Aerospace Engineering  
Korea Advanced Institute of Science and Technology  
Daejeon, 305-701, Korea

**Byung-Eul Jun\*\*\* and Jin-ik Lee\*\*\***

Guidance and Control Directorate  
Agency for Defense Development, Daejeon, 305-152, Korea

## Abstract

In this work, we explore the feasibility of roll-pitch-yaw integrated autopilots for high angle-of-attack missiles. An investigation of the aerodynamic characteristics of a surface-to-air missile is presented, which reveals the strong effects of cross coupling between the longitudinal and lateral dynamics. Robust control techniques based on  $H_\infty$  synthesis are employed to design roll-pitch-yaw integrated autopilots. The performance of the proposed roll-pitch-yaw integrated controller is tested in high-fidelity nonlinear five-degree-of-freedom simulations accounting for kinematic cross-coupling effects between the lateral and longitudinal channels. Against nonlinearity and cross-coupling effects of the missile dynamics, the integrated controller demonstrates superior performance when compared with the controller designed in a decoupled manner.

**Key Word** : Autopilot, High angle-of-attack missile, Robust control

## Introduction

In designing control systems for various mobile systems such as cars, aircraft, helicopters, and missiles, it is often assumed that dynamics in the longitudinal direction and lateral direction are independent of each other. This assumption leads to decoupled dynamic models, which allows a much simpler control design process. However, this assumption is not always reasonable. Also, in order to extend the applicable region of the controller and thus to utilize the operation capacity of the system under control consideration of the overall coupled dynamics is often necessary.

There have been research activities to design an integrated controller for missiles, rather than separate controllers for longitudinal and lateral channels. In [1], a backstepping controller is presented for the coupled lateral and longitudinal dynamics of an air-to-air missile. Although the robustness analysis with respect to the aerodynamic uncertainties was attempted, it is difficult to systematically

---

\* Graduate Student

\*\* Assistant Professor

E-mail : hjinkim@snu.ac.kr

TEL : (82)2-880-9252

FAX : (82)2-887-2662

\*\*\* Principal researcher, Agency for Defense Development

analyze how a certain design choice affects the closed-loop robustness using this approach. Also, PID-type controller gains have been obtained using the co-evolutionary augmented Lagrangian methods for the coupled dynamics of a surface-to-air missile [2]. However, it is difficult to formally provide the closed-loop robustness against perturbation or disturbance using such an approach.

On the other hand, robust control theories such as  $H_\infty$  and  $\mu$ -synthesis provide a formal framework to allow systematic robustness analysis and synthesis of a robust controller [6,7]. For a decoupled model, the autopilot of a bank-to-turn missile with very lightly damped bending modes is synthesized using the  $H_\infty$  loop-shaping design procedure [3]. Robustness against large modeling uncertainties including parameters and bending modes is investigated. In [4], employing  $\mu$ -synthesis, separate controllers for the lateral dynamics and the roll dynamics have been designed, respectively. In addition, a conditioning/blending technique is introduced to schedule the controllers over the entire flight envelope as a function of dynamic pressure. The resulting autopilot is evaluated in nonlinear simulation. Also, the paper illustrates a practical application of advanced control techniques in a realistic environment. A gain-scheduled autopilot design for a bank-to-turn missile is presented in [5]. Instead of linearizing the dynamics about the operating points, the missile dynamics are represented in a linear parameter varying form. Separate controllers for pitch and roll/yaw channels were designed at fixed points using  $\mu$ -synthesis, and a switching gain scheduler was simulated with a nonlinear missile model. In [8], three controllers for the coupled dynamics of a bank-to-turn missile have been presented, which are the linear quadratic gaussian(LQG) method, generalized singular linear quadratic(GSLQ) method, and  $H_\infty$  method using Hamiltonian approach. The robust performance of each design is tested, which shows a good response against aerodynamic variations and significant kinematic and inertia coupling. Two approaches to nonlinear robust control design are examined in [9]. The first approach is an input/output linearized robust controller design, and the second approach uses a recursive or backstepping design procedure to derive a nonlinear controller. Both controllers stabilize the system in the presence of large uncertainties, but robust recursive controller demonstrates significant performance improvements over input/output linearized robust controller.

In this research, the  $H_\infty$  loop-shaping controller is designed for a 5 degree of freedom (DOF) model of a surface-to-air missile. In the next section, a 5-DOF model is obtained by fixing a longitudinal velocity in a full 6-DOF nonlinear dynamics. The corresponding aerodynamic coefficients are analyzed to observe cross-coupling effects caused by simultaneous pitch and yaw maneuvering and justify the necessity of the combined longitudinal/lateral design for high angle of attack missiles. Then, a  $H_\infty$ -control design problem is formulated for the application to the missile autopilot, followed by a description of the detailed design process. Both linear and nonlinear simulation results are presented in order to verify the performance of the proposed controller. Last section concludes the paper with future directions.

## Missile Model

This section describes the differential equations for the surface-to-air missiles under consideration and actuator dynamics.

### 5-DOF Missile Dynamics

Standard six-degree-of-freedom (6-DOF) equations of motion for a missile with an axisymmetric configuration in the body coordinate frame can be written as

$$\begin{aligned}
 \dot{u} &= vr - wq - g \sin \theta + F_x / m \\
 \dot{v} &= wq - ur + g \sin \phi \cos \theta + F_y / m \\
 \dot{w} &= uq - vp + g \cos \phi \cos \theta + F_z / m \\
 \dot{p} &= M_x / I_{xx} \\
 \dot{q} &= \{(I_{zz} - I_{xx})pr + M_y\} / I_{yy} \\
 \dot{r} &= \{(I_{xx} - I_{yy})pq + M_z\} / I_{zz}
 \end{aligned} \tag{1}$$

where  $m$  is mass,  $I_{xx}$ ,  $I_{yy}$ ,  $I_{zz}$  are the moment of inertia,  $(u, v, w)$  are the velocity components and  $(p, q, r)$  denote the corresponding angular rates.  $(F_x, F_y, F_z)$  and  $(M_x, M_y, M_z)$  represent the aerodynamic forces and moments, respectively.

The aerodynamic forces and moments are determined by the following equations :

$$\begin{aligned} F_x &= -QS(C_x + C_{xb}) + ma_T \\ F_y &= QSC_y \\ F_z &= QSC_z \\ M_x &= QSD\left(C_l + \frac{D}{2V_m} C_{lp}P\right) \\ M_y &= QSD\left(C_m + \frac{D}{2V_m} C_{mq}q\right) \\ M_z &= QSD\left(C_n + \frac{D}{2V_m} C_{nr}r\right) \end{aligned} \quad (2)$$

where  $Q$  is dynamic pressure,  $S$  is the reference area,  $D$  is the diameter of the missile,  $V_m$  is velocity, and  $a_T$  is thrust. Aerodynamic coefficients,  $C_x, \dots, C_{nr}$ , are provided by an aerodynamic coefficient module based on the flight data. They are functions of altitude, Mach, angle of attack  $\alpha$ , side slip angle  $\beta$ , and fin deflection  $\delta$ .

We define the 5-DOF models by fixing the altitude and X-direction velocity from the nonlinear 6-DOF models. For propulsion-gliding solid propellant missiles, the cross-coupling effects with roll-pitch-yaw channels and nonlinear properties could be conserved even if the longitudinal velocity, which changes slowly and uncontrollable, is fixed.

By assuming that the missile is rigid body, has cruciform symmetrical properties, and performs gliding maneuver after combustion, Eq. (1) may be written as

$$\begin{aligned} \dot{v} &= wp - u_0 r + g \sin \phi \cos \theta + F_y/m \\ \dot{w} &= u_0 q - vp + g \cos \phi \cos \theta + F_z/m \end{aligned} \quad (3)$$

## Model Analysis

As mentioned in the previous section, the aerodynamic models used in this work can be written as the function of flight condition and control surface deflections. The aerodynamic coefficients extracted from an aerodynamic module are used to calculate forces and moments. In order to carry out an initial investigation on aerodynamic characteristics, we represent the variations of aerodynamic coefficients according to Mach number,  $\alpha$ ,  $\beta$  and control deflections.

When the control inputs are zero, the variation of  $C_l$  vs. roll angle  $\phi$  at various  $\alpha$  and Mach numbers are given in Fig. 1. The induced roll moment coefficient appear to be trigonometrical functions with the period of  $90^\circ$ , showing the peak values at  $22.5^\circ$  and  $67.5^\circ$ . The smaller Mach number is, the larger peak value becomes. Accordingly, not only the consequence of these effects would deteriorate the missile's performance, but it can give rise to unexpected dynamic characteristics.

Fig. 2 shows the induced roll moment coefficient as  $\alpha$  is varied from  $0^\circ$  and  $20^\circ$ , with a constant bank angle at 0, 5, 10, 20 degrees. It can be seen that the coefficient is large at a low Mach number and large sideslip angle region.

The effects of roll control inputs on the missile model are shown in Fig. 3 and Fig. 4. Fig. 3 shows the plots of  $C_l$  versus roll control  $\delta_r$  at each value of  $\beta$  and Mach number, when  $\alpha=10^\circ$ . Fig. 4 shows the similar plots when  $\alpha=20^\circ$ . It should be noted that the roll moments can be generated without roll control inputs when  $\alpha$  is nonzero. Especially, when the missile maneuvers in the low Mach number and high angle-of-attach region, these issues are noticeable (see Fig. 4(a), for example). These kinematic cross-coupling effects caused by simultaneous pitch and yaw maneuvering make the control problem more difficult.

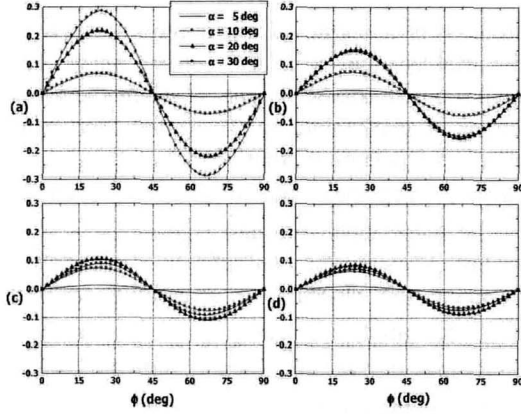


Fig. 1. The plot of  $C_l$  versus  $\phi$  at (a) Mach = 1.5, (b) Mach = 2.0, (c) Mach = 2.5, and (d) Mach = 3.0

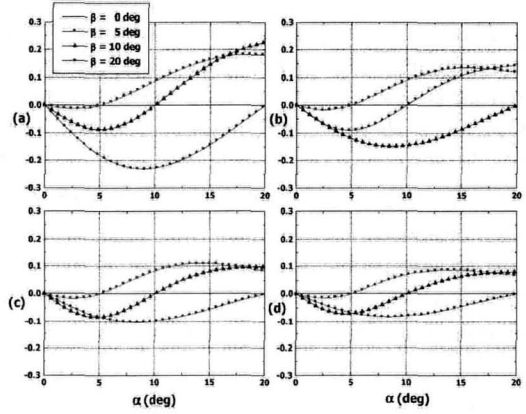


Fig. 2. The plot of  $C_l$  versus  $\alpha$  at (a) Mach = 1.5, (b) Mach = 2.0, (c) Mach = 2.5, and (d) Mach = 3.0

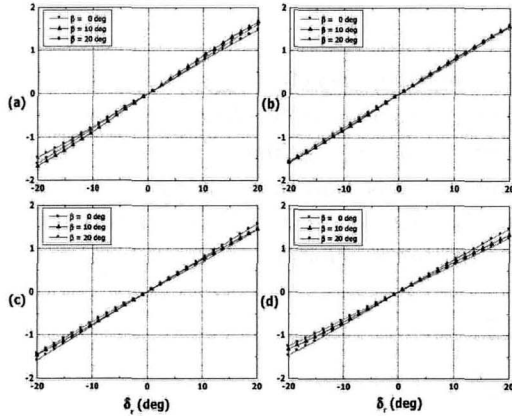


Fig. 3. The plot of  $C_l$  versus  $\delta_r$  with  $\alpha = 10^\circ$  at (a) Mach = 1.5, (b) Mach = 2.0, (c) Mach = 2.5, and (d) Mach = 3.0

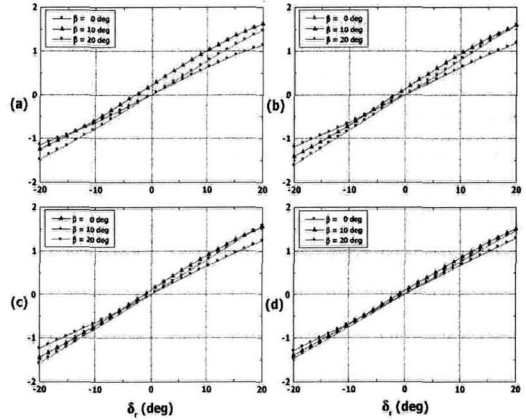


Fig. 4. The plot of  $C_l$  versus  $\delta_r$  with  $\alpha = 20^\circ$  at (a) Mach = 1.5, (b) Mach = 2.0, (c) Mach = 2.5, and (d) Mach = 3.0

## Robust control based on $H_\infty$ -theory

In order to design a robust controller for the coupled dynamics with the cross-coupling effects described in the previous section,  $H_\infty$  synthesis is employed. This section addresses the problem formulation in the  $H_\infty$  framework.

One modern approach to characterizing closed-loop performance objectives is to measure the size of certain closed-loop transfer function matrices using various matrix norms. Matrix norms provide a measure of how large output signals can become for certain classes of input signals. Optimizing these types of performance metrics over the set of stabilizing controllers is the main thrust of recent optimal control theory, such as  $L_1$ ,  $H_2$ ,  $H_\infty$ , and  $\mu$ -synthesis.

We employ a synthesis technique based on the  $H_\infty$ -optimal control, whose general formulation is afforded by the configuration shown in Fig. 5. Here  $G$  is a generalized plant and  $K$  is a feedback controller. The generalized plant  $G$  contains what is usually called the nominal plant

and design-specific weighting functions. The signal  $w$  contains all external inputs, including disturbances, sensor noise, and commands. The output  $z$  is a signal of our interests, such as error signals or control efforts.  $v$  is the measured variables, and  $u$  is the control input. The diagram is also referred to as a linear fractional transformation on  $\Delta$ ,  $K$ , and  $G$ . Here the block  $\Delta$  includes all possible dynamic/parametric perturbations or uncertainty in the system. By using suitable normalization, it is usually assumed without loss of generality that  $\|\Delta\|_\infty \leq 1$ .

Throughout this paper, we formulate closed-loop performance objectives as  $H_\infty$ -norm of weighted closed-loop transfer functions, which are to be made small through feedback.

In our problem, Fig. 5 can be converted into Fig. 6 using the multiplicative uncertainty representation. The objective of  $H_\infty$  control is to make the closed-loop sensitivity transfer function, denoted by  $T_{ed}$  that is presented in Fig. 6, satisfy  $\|T_{ed}\|_\infty \leq 1$ . Performance requirements on the closed-loop system are transformed into the  $H_\infty$  framework with the help of weighting or scaling functions. They are used to scale the input/output transfer functions such that when  $\|T_{ed}\|_\infty \leq 1$ , the relationship between the external input and the error is suitable. These design choices should account for the relative magnitude of signals, their frequency dependence, and their relative importance.

The transfer function matrices are defined as

$$\text{Transfer Function}_{z_1 \rightarrow w_1} = T_I = KG(I + GK)^{-1} \tag{6}$$

where  $T_I$  denotes the input complementary sensitivity function. To ensure that the closed-loop system is robust to multiplicative uncertainty,  $\Delta_M$ , around the plant  $G$ , it give bounds on the size of the transfer function matrices from  $z_1$  to  $w_1$ . In the  $H_\infty$  control problem formulation, the robustness objectives enter the synthesis procedure as additional input/output signals to be kept small. The  $H_\infty$  control robustness objective is now in the same format as the performance objectives, that is, to minimize the  $H_\infty$  norm of the transfer matrix from  $z_1$  to  $w_1$ .

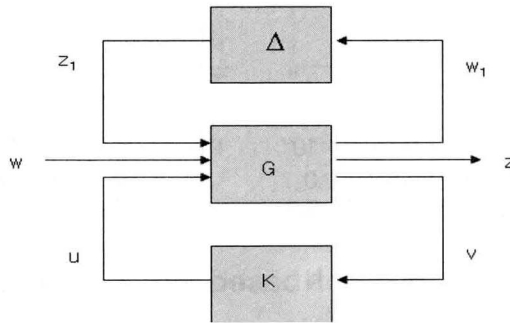


Fig. 5. General control configuration for the case with model uncertainty

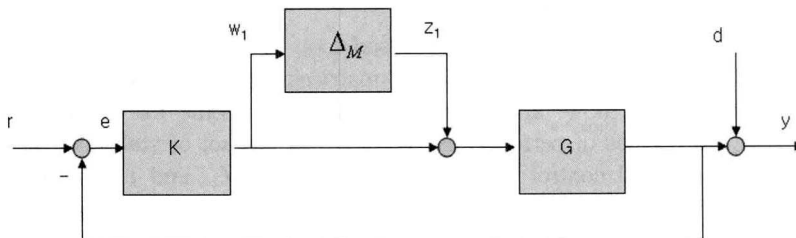


Fig. 6. Closed-loop feedback system with multiplicative uncertainty model

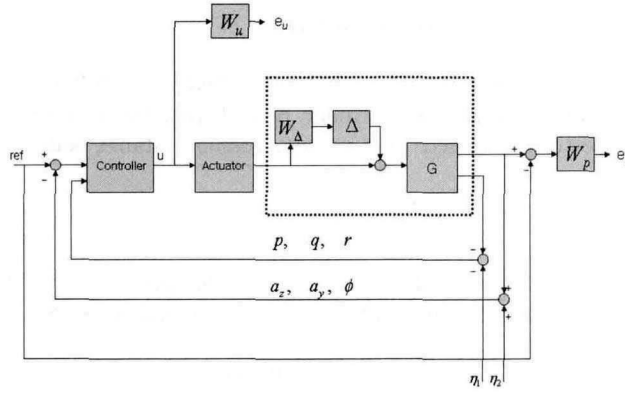


Fig. 7. Interconnection structure for the roll-pitch-yaw integrated autopilot

Weighting or scaling matrices are often introduced to shape the frequency and magnitude content of the sensitivity and complementary sensitivity transfer function matrices. Let  $W_M$  correspond to the multiplicative uncertainty.  $\Delta_M$  are assumed to be a norm bounded by 1, that is,  $|\Delta_M(s)| < 1$ . Hence as a function of frequency,  $|W_M(j\omega) \text{RIGHT}|$  are the respective sizes of the largest anticipated multiplicative plant perturbations. The multiplicative weighting or scaling  $W_M$  represents a percentage error in the model and is often small in magnitude at low frequency, frequency, between 0.05 and 0.2 (5% to 20% modeling error), and growing larger in magnitude at high frequency, 2 to 5 (200% to 500% modeling error). The weight will transition by crossing a magnitude value of 1, which corresponds to 100% uncertainty in the model, at a frequency at least twice the bandwidth of the closed-loop system.

The objective is to design an  $H_\infty$  optimal control law for system interconnection structure given by the block diagram in Fig. 7.

## Design Process

### Linearization of the nonlinear missile dynamics

The  $H_\infty$ -synthesis of missile control systems begins with the development of a linearized model of the missile. By assuming that the missile performs a gliding maneuver after the boosting phase, we execute the linearization of the nonlinear missile dynamics of Eqs. (1)-(5).

Then we arrive at the following linearized 5-DOF model in terms of  $[w \ q \ v \ p \ r \ \phi]^T$ , and control inputs  $U = [\delta_r \ \delta_z \ \delta_y]^T$ :

$$\begin{bmatrix} \dot{w} \\ \dot{q} \\ \dot{v} \\ \dot{p} \\ \dot{r} \\ \dot{\phi} \end{bmatrix} = \begin{bmatrix} a_{11} & a_{12} & a_{13} & a_{14} & 0 & 0 \\ a_{21} & a_{22} & a_{23} & a_{24} & 0 & 0 \\ a_{31} & 0 & a_{33} & a_{34} & a_{35} & 0 \\ a_{41} & 0 & a_{43} & a_{44} & 0 & 0 \\ a_{51} & 0 & a_{53} & a_{54} & a_{55} & 0 \\ 0 & 0 & 0 & 1 & 0 & 0 \end{bmatrix} \begin{bmatrix} w \\ q \\ v \\ p \\ r \\ \phi \end{bmatrix} + \begin{bmatrix} b_{11} & 0 & 0 \\ b_{21} & 0 & 0 \\ 0 & 0 & b_{33} \\ b_{41} & b_{42} & b_{43} \\ 0 & 0 & b_{53} \\ 0 & 0 & 0 \end{bmatrix} \begin{bmatrix} \delta_r \\ \delta_z \\ \delta_y \end{bmatrix} \quad (7)$$

$$\begin{bmatrix} \phi \\ p \\ q \\ r \\ a_z \\ a_y \end{bmatrix} = \begin{bmatrix} 0 & 0 & 0 & 0 & 0 & 1 \\ 0 & 0 & 0 & 1 & 0 & 0 \\ 0 & 1 & 0 & 0 & 0 & 0 \\ 0 & 0 & 0 & 0 & 1 & 0 \\ c_{51} & 0 & c_{53} & 0 & 0 & 0 \\ c_{61} & 0 & c_{63} & 0 & 0 & 0 \end{bmatrix} \begin{bmatrix} w \\ q \\ v \\ p \\ r \\ \phi \end{bmatrix} + \begin{bmatrix} 0 & 0 & 0 \\ 0 & 0 & 0 \\ 0 & 0 & 0 \\ 0 & 0 & 0 \\ d_{51} & 0 & 0 \\ 0 & 0 & d_{63} \end{bmatrix} \begin{bmatrix} \delta_r \\ \delta_z \\ \delta_y \end{bmatrix} \quad (8)$$

We omit the specific values in these linearized equations of motion.

## $H_\infty$ Synthesis for the 5-DOF missile dynamics

The interconnection structure for  $H_\infty$  controller design is shown in Fig. 7. The control design objective is to design a stabilizing controller  $K$  such that for all stable perturbations  $\Delta(s)$ , with  $\|\Delta\|_\infty < 1$ , the perturbed closed-loop system remains stable, and satisfies the following performance criterion:

$$\left\| \begin{array}{c} W_p(I+GK)^{-1} \\ W_u K(I+GK)^{-1} \end{array} \right\|_\infty < 1$$

The interconnection structure for the roll-pitch-yaw integrated autopilot is shown in Fig. 5. We consider the input multiplicative uncertainty  $W_\Delta$  represented by

$$W_\Delta(s) = 50 \frac{(s+100)}{(s+10000)},$$

so that the uncertain plants are expressed as  $\{G(1+\Delta W_\Delta): \Delta \text{ stable, } \|\Delta\|_\infty < 1\}$ , where  $G$  is a transfer function of the nominal plant. This type of uncertainty is called multiplicative uncertainty at the plant input. The transfer function  $W_\Delta$  is assumed known, and reflects the amount of uncertainty in the model.

Thus the transfer function  $W_\Delta$  is chosen to represent a frequency-dependent magnitude bound on the unmodeled dynamics. This particular choice of  $W_\Delta(s)$  was taken directly from reference[6].

The performance of the closed loop system will be evaluated using the  $H_\infty$  norm of the output sensitivity transfer function,  $(I+GK)^{-1}$ .

The  $W_p$  and  $W_u$  blocks are the performance and control weighting functions, respectively, which are chosen as

$$W_p(s) = \frac{(s/Z^{1/n} + w_B)^n}{(s + w_B A^{1/n})^n}, \quad W_u(s) = 10^{-5},$$

where  $Z=0.15$ ,  $w_B=30$ ,  $A=10^{-4}$ , and  $n=2$ . These weighting functions are selected by trial and error from reference[6].

We can say that nominal performance is achieved if  $\|W_p(I+GK)^{-1}\|_\infty < 1$ . As in the uncertainty modeling, the weighting function  $W_p$  is used to normalize specifications, in this case, to define performance as whether a particular norm is less than 1. In order to achieve  $\|W_p(I+GK)^{-1}\|_\infty < 1$ , the maximum singular value plot of the sensitivity transfer function  $(I+GK)^{-1}$  must lie below the plot of  $1/|W_p|$  at every frequency.

In Fig. 8, we show the frequency response of the inverse weighting function  $W_p^{-1}$ .

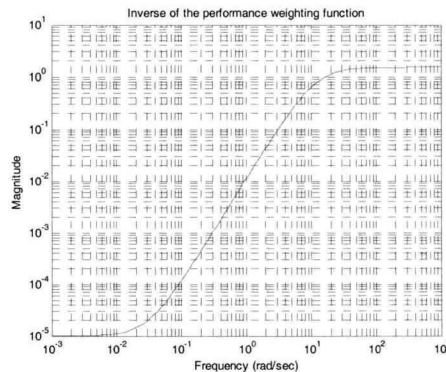


Fig. 8. Frequency response of the inverse weighting function



## Simulation Results

In this section, we verify the performance and robustness of the roll-pitch-yaw integrated controller, using both linear and nonlinear simulations. All the responses presented here were simulated using the controller designed at Mach = 2.0,  $a_z = -5g$ , and  $a_y = 5g$ .

To simulate the integrated autopilots, the missile have imposed on a simultaneous step command of  $a_z$ ,  $a_y$ , and  $\phi$ . Fig. 9 shows the linear simulation results to the step command and Fig. 10 shows the control inputs used in the linear simulation. Results indicates that satisfactory performance is obtained and the all the state variables and commands remain within the design specifications on the saturation limits of 30 degrees and 450 deg/sec. On the other hand, the controller designed based on the decoupled longitudinal and lateral dynamics fails to achieve stable responses against the coupled dynamics.

Fig. 11 shows the simulation results of the integrated controller with the nonlinear 5-DOF missile model trimmed at  $M=2.0$ ,  $a_z = -5g$ , and  $a_y = 5g$ , and the same step commands as Fig. 9. And Fig. 12 displays the control inputs used in the nonlinear simulation. It can be seen from comparing Fig. 9 and Fig. 11 that there is a slight increase in the overshoot of  $a_z$ , and  $a_y$ , Also, the roll-rate response in Fig. 11 shows a chattering, which is not observed in the linear simulation.

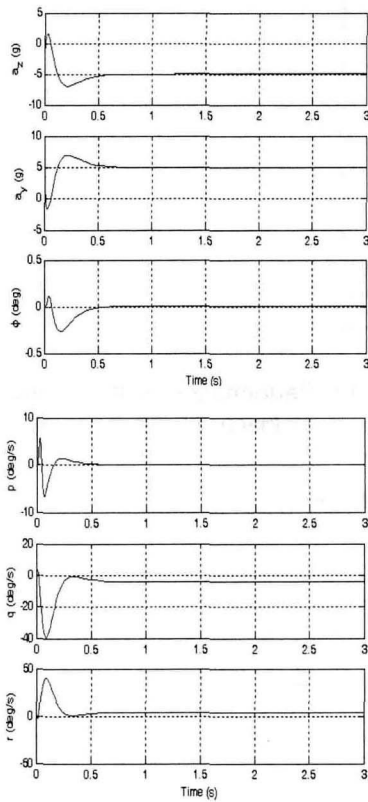


Fig. 9. Linear simulation result: State variables under the controller designed at Mach 2.0,  $a_z = -5$ ,  $a_y = 5$

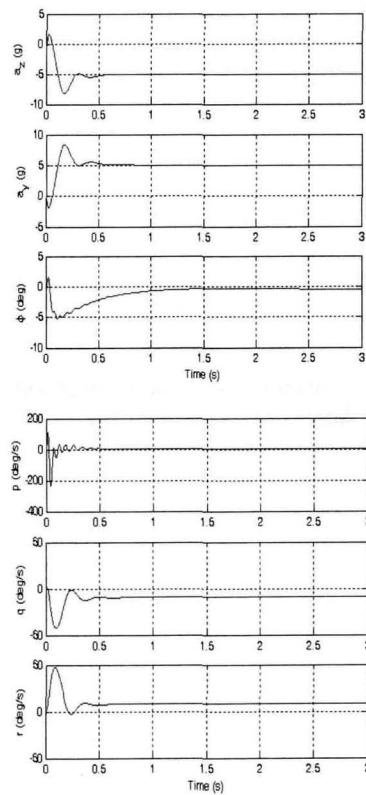


Fig. 11. Nonlinear simulation result: State variables under the controller designed at Mach 2.0,  $a_z = -5$ ,  $a_y = 5$



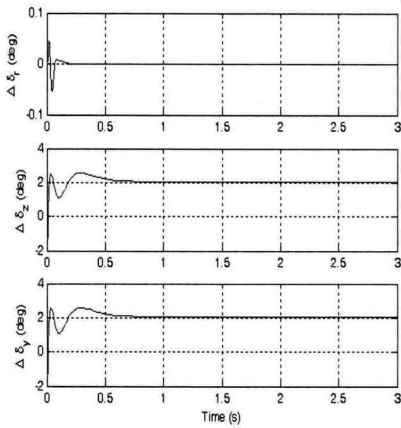


Fig. 10. Linear simulation result: Control inputs of the controller designed at Mach 2.0,  $a_z = -5$ ,  $a_y = 5$

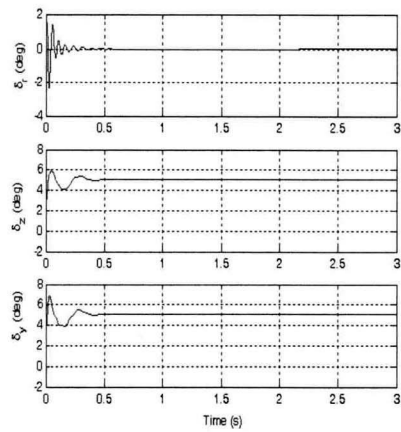


Fig. 12. Nonlinear simulation result: Control inputs of the controller designed at Mach 2.0,  $a_z = -5$ ,  $a_y = 5$

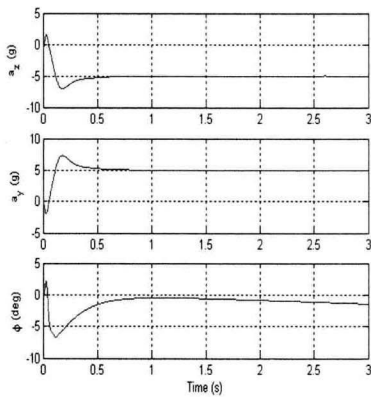


Fig. 13. Performance of the controller at Mach 2.0  $a_z = -10$ ,  $a_y = 10$

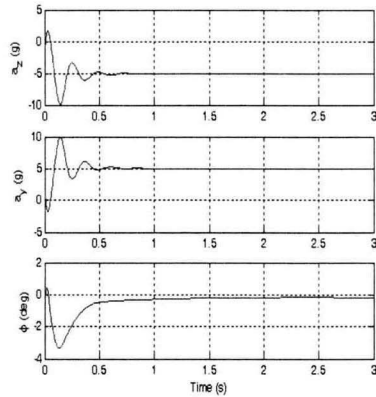


Fig. 14. Performance of the controller at Mach 3.0  $a_z = -5$ ,  $a_y = 5$

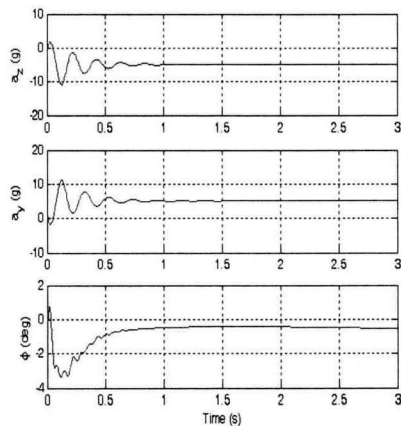


Fig. 15. Performance of the controller at Mach 3.0  $a_z = -10$ ,  $a_y = 10$

In order to investigate the robustness of the proposed controllers, we apply the controller to the plant trimmed at different points. Fig. 13 shows the step responses of the missile trimmed at Mach 2.0,  $a_z = -10g$ , and  $a_y = 10g$ , using the controller designed at  $M=2.0$ ,  $a_z = -5g$ , and  $a_y = 5g$ . Fig. 14 is the step responses with Mach 3.0,  $a_z = -5g$ , and  $a_y = 5g$  and Fig. 15 shows the step responses with Mach 3.0,  $a_z = -10g$ , and  $a_y = 10g$ . It indicates that the performance of the designed controller is satisfactory over the wide operating range.

## Conclusions

In this research, following the investigations of the aerodynamic characteristics for surface-to-air missile, which reveal strong cross-coupling effects between the longitudinal and lateral dynamics, we designed roll-pitch-yaw integrated autopilots for the pitch/yaw acceleration and roll angle tracking problem based on the  $H_\infty$ -control techniques. The designed autopilot is evaluated in a fully nonlinear 5-DOF simulation. The results showed that the proposed controller performs well in terms of the stabilizing performance when the nonlinearities and cross-coupling effects dominate the missile dynamics. Furthermore, the integrated  $H_\infty$ -controller with input multiplicative uncertainty achieved the satisfactory command tracking performance and showed robustness in a wide flight envelope. Future research includes a gain-scheduling problem to cover a full envelope. Realistic engagement scenarios will be employed to demonstrate the performance and robustness properties of the proposed autopilots.

## Acknowledgement

This work was supported by Agency for Defense Development under the contract UD060056ED.

## References

1. Dahlgren, J., 2002, "Robust nonlinear control design for a missile using backstepping", *Master's thesis*, Linkoping Univ.
2. Jeon, B. and Lee, J., 2007, "Missile Autopilot Design Based on 5-DOF Models", *Proceeding of the KSAS Fall Conference*, Cheju, pp. 1109-1112
3. Friang, J., Duc, G. and Bonnet, J., 1998, "Robust autopilot for a flexible missile: Loop-shaping  $H_\infty$  design and real  $\mu$ -analysis", *J. of Robust and nonlinear Control*, Vol. 8, pp. 129-153
4. Buschek, H., 1999, "Full Envelop Missile Autopilot Design using Gain Scheduled Robust Control", *J. of Guidance, Control, and Dynamics*, Vol. 22, No. 1
5. Carter, L. and Shamma, J., 1996, "Gain-Scheduled Bank-to-Turn Autopilot Design Using Linear Parameter Varying Transformation", *J. of Guidance, Control, and Dynamics*, Vol. 19, No. 5
6. Skogestad, S. and Postlethwaite, I., 2003, *Multivariable feedback control*, John Wiley & Sons, New York.
7. Doyle, J. C. and Zbou, K., 1998, *Essential of robust control*, Prentice Hall, New Jersey.
8. Lin, C. F., Clutier, J. R. and Evers J. H. 1995, "Robust Bank-to-Turn Missile Autopilot Design", *Proceeding of the American Control Conference*, Seattle, pp. 1941-1945
9. Hull, R. A., 1995, "Design and Evaluation of Robust Nonlinear Missile Autopilots from a Performance Perspective", *Proceeding of the American Control Conference*, Seattle, pp. 189-193